RESEARCH ARTICLE | JANUARY 14 2019

# Terahertz photoconductive emitter with dielectric-embedded high-aspect-ratio plasmonic grating for operation with low-power optical pumps

**Special Collection:** 2019 Photonics and Optics

D. V. Lavrukhin; A. E. Yachmenev; I. A. Glinskiy; R. A. Khabibullin; Y. G. Goncharov; M. Ryzhii ; T. Otsuji ; I. E. Spector; M. Shur ; M. Skorobogatiy; K. I. Zaytsev ; D. S. Ponomarev



*AIP Advances* 9, 015112 (2019)
https://doi.org/10.1063/1.5081119







# Terahertz photoconductive emitter with dielectric-embedded high-aspect-ratio plasmonic grating for operation with low-power optical pumps

Cite as: AIP Advances 9, 015112 (2019); doi: 10.1063/1.5081119
Submitted: 14 November 2018 • Accepted: 26 December 2018 •
Published Online: 14 January 2019



D. V. Lavrukhin,[1,2] A. E. Yachmenev,[1,2] I. A. Glinskiy,[3] R. A. Khabibullin,[1,2,4] Y. G. Goncharov,[2] M. Ryzhii,[5] T. Otsuji,[6] I. E. Spector,[2] M. Shur,[7,8] M. Skorobogatiy,[9] K. I. Zaytsev,[2,10] and D. S. Ponomarev[1,2,4,a)]

## AFFILIATIONS

[1] Institute of Ultra High Frequency Semiconductor Electronics of RAS, Moscow 117105, Russia
[2] Prokhorov General Physics Institute of the Russian Academy of Sciences, Moscow 119991, Russia
[3] Moscow Technological University (MIREA), Moscow 119454, Russia
[4] Center of Photonics and 2D Materials, Moscow Institute of Physics and Technology, Dolgoprudny 141700, Russia
[5] Department of Computer Science, University of Aizu, Aizu-Wakamatsu 965-8580, Japan
[6] Research Institute of Electrical Communication, Tohoku University, Sendai 980-8577, Japan
[7] Rensselaer Polytechnic Institute, Troy, New York 12180, USA
[8] Electronics of the Future, Inc., Vienna, Virginia 22181, USA
[9] Department of Engineering Physics, Polytechnique Montreal, Montreal, Quebec H3T 1J4, Canada
[10] Bauman Moscow State Technical University, Moscow 105005, Russia

[a)] **Electronic mail**: ponomarev_dmitr@mail.ru



## ABSTRACT

We report on the design, optimization and fabrication of a plasmon-assisted terahertz (THz) photoconductive antenna (PCA) for THz pulse generation at low-power optical pumps. The PCA features a high aspect ratio dielectric-embedded plasmonic Au grating placed into the photoconductive gap. Additionally, $Si_3N_4$-passivation of the photoconductor and the $Al_2O_3$-antireflection coating are used to further enhance antenna performance. For comparative analysis of the THz photocurrents, THz waveforms and THz power spectra we introduced the THz photocurrent $\delta_i$ and the THz power enhancement $\delta_{THz}$ factors, which are defined as ratios between the THz photocurrents and the THz power spectra for the plasmon-assisted and conventional PCAs. We demonstrated superior performance of the plasmon-assisted PCA $\delta_i$=30 and $\delta_{THz}$=3 · $10^3$ at the lowest optical pump power of $P$=0.1 mW. Nevertheless the increase to $P$=10 mW lead to monotonically decrease in the both values to $\delta_i$=2 and $\delta_{THz}$=$10^2$ due to screening effects. These results demonstrate a strong potential of the plasmonic PCA for operation with low-power lasers, thus, opening opportunities for the development of portable and cost-effective THz spectrometers and imaging systems.



Existing THz sources do not meet many challenges posed by the rapidly-developing THz science and technology[1] and improving the efficiency of the THz emitters remains a difficult problem. The photoconductive antennas (PCAs) based either on photoswitching[2,3] or photomixing[4,5] effects, are the prevalent THz emitters widely used in the THz spectroscopy

and imaging due to the their reliability, cost effectiveness and a relative ease of fabrication. Since the first experimental observation of photo switching in semiconductors,[6] rapid progress in the THz PCA technology has been achieved by using different materials and semiconductor technologies.[7–9] Nevertheless, enhancement of the optical-to-THz-wave conversion efficiency and development of the THz PCAs operating with low-power optical pumps remain a challenge.

Recently, an approach for boosting the THz PCAs performance using plasmonic or dielectric nanoantennas incorporated into a photoconductive gap has been proposed.[10,11] In such PCAs, strong confinement of the optical pump excitation at the semiconductor/nanoantenna interface leads to enhancement of the light matter interaction, and to improvement of the antenna thermal efficiency.[12–14] The PCA-emitters and PCA-detectors using different geometries of metal and dielectric nanoantennas, such as silver nano-islands or arrays of nanoscale apertures,[15–17] fractal antennas,[18] monopole or dipole plasmonic gratings with either low or high aspect ratios,[10,11,19–24] plasmonic nanocavities based on Bragg reflectors,[25] metal colloidal particles deposited onto the photoconductive substrate,[26] or even all-dielectric gratings,[27] demonstrated impressive performance enhancement compared to the conventional PCAs.

In this paper, we report on a plasmon-assisted THz PCA that enhances the THz pulse generation and operates with low-power optical pumps. The THz wave generation enhancement is due to a favorable combination of a high aspect ratio dielectric-embedded plasmonic Au grating (resulting in a stronger optical field - photoconductor interaction), a $Si_3N_4$-passivation layer (that significantly reduces leakage currents and sustains thermal stability of the PCA), as well as an $Al_2O_3$-antireflection and protection coating (that reduces the Fresnel losses of the photoconductive gap and promotes the mechanical stability of the grating). For comparison, a conventional PCA was also fabricated. We demonstrated superior performance of the plasmon-assisted PCA which THz photocurrent and THz power spectrum were 30 and $3 \cdot 10^3$ higher than those of a conventional PCA at the lowest optical pump power of P=0.1 mW, thus confirming that our plasmonic PCA is well suited for operation with low-power lasers. We believe that the plasmonic PCA reported in this work could become a key enabling component in the upcoming portable and cost-effective THz spectrometers and imaging systems.

Figures 1 (a) and (b) show the respective schematics of the studied plasmon-assisted PCA and the high-aspect-ratio dielectric embedded Au-grating in the PCA's gap. The PCA features log-spiral Au-electrodes on a semi-insulating GaAs (SI-GaAs) photoconductive substrate. In order to significantly reduce the dark current, the photoconductor was passivated using a $Si_3N_4$-film with the windows for Ti/Au metallization etched prior to the plasmonic grating deposition. The plasmonic antenna is made of two physically spaced plasmonic gratings. In turn, each grating features an array of Au-nanoridges with rectangular cross-sections placed

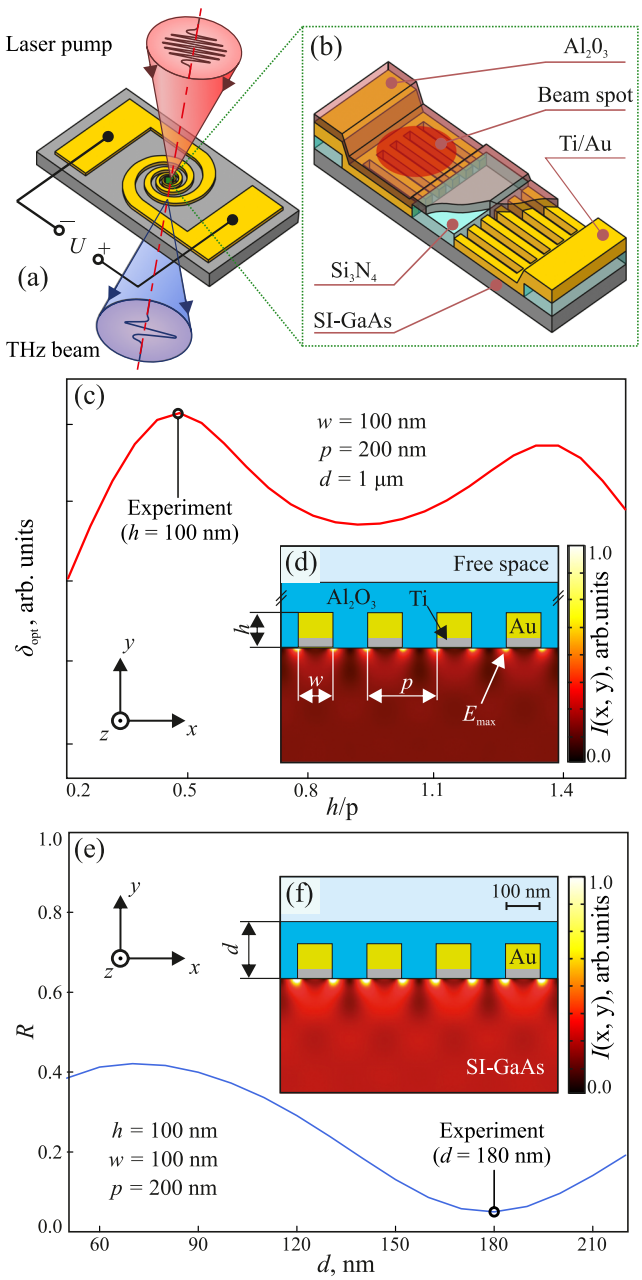


**FIG. 1.** Schematics of (a) the antenna design; (b) the gap region of a plasmonic PCA; (c) simulated local optical intensity enhancement factor $\delta_{opt}$ as a function of the Ti/Au-grating height-to-period with semi-infinite $Al_2O_3$-coating ($d$=1 $\mu$m in simulation); (d) optical field intensity $I(x, y)$ in the photoconductor layer with semi-infinite $Al_2O_3$-coating and Ti/Au-grating height of $h$= 100 nm, width of $w$= 100 nm and period of the grating $p$= 200 nm; (e) simulated PCA reflectivity $R$ at $\lambda = 0.78\mu$m as a function of the $Al_2O_3$-coating thickness $d$; (f) optical field intensity $I(x, y)$ in the photoconductor layer for $h$= 100 nm, $w$= 100 nm, $p$= 200 nm and $d$= 180 nm.

periodically onto the photoconductive substrate and brought in contact with the corresponding PCA electrodes. Finally, the antenna is covered with an $Al_2O_3$-coating, which infiltrates the

gaps between the Au-nanoridges The PCA is pumped using a femtosecond laser beam focused onto the anode plasmonic grating (see Fig. 1 (b)).

The proposed plasmonic PCA enhances THz pulse generation due to strong field confinement at the interface between the plasmonic grating and the semiconductor material.[14] In order to optimize PCA geometry, we performed numerical simulations using finite-element method of solving the Maxwell's equations by COMSOL Multiphysics.[28,29] The values of the material optical parameters were taken from the existing literature - SI-GaAs,[30] Au,[31] and $Al_2O_3$.[32]

In our simulations, we used a monochromatic plane wave of $\lambda = 0.78\mu$m incident normally at the PCA. To achieve an efficient excitation of the plasmonic modes of the metal grating, the incident plane wave polarization was chosen to be perpendicular to the Au-nanoridges.[10] Furthermore, we used the semi-infinite SI-GaAs substrate, the individual nanoridge width of $w$= 100 nm, and the grating period of $p$= 200 nm, while the plasmonic grating height $h$ and the $Al_2O_3$-coating thickness $d$ were varied to achieve an optimal design. Figures 1 (d), (f) present the numerically simulated spatial distributions of the electromagnetic (EM) field intensity $I(x, y)$ in the photoconductor. These plots show that the antireflection coating leads to a significant enhancement of the field intensity in the plasmonic grating modes (the same scale is used for the two-color bars in Figs. 1 (d) and (f)).

Figure 1 (c) shows the local optical field intensity enhancement factor $\delta_{opt} = |E_{max}|^2/|E_0|^2$ as a function of the Au-nanoridge height $h$ with with the semi-infinite $Al_2O_3$-coating (1 $\mu$m in the simulation). Here $E_{max}$ is the maximal local amplitude of the electric field at the shadow side of the plasmonic Ti/Au grating (we used the thickness of Ti equal to 18 nm) and $E_0$ is the amplitude of the homogeneous electric field formed in the photoconductive substrate without the Au-nanoridges. The higher is the value of $\delta_{opt}$, the higher will be the absorbed local optical pump intensity, thus contributing to the generation of the electron-hole pairs and, therefore, to the THz photocurrent and to the THz pulse generation.[14]

Figure 1 (c) shows that, at first, $\delta_{opt}$ increases reaching its maximum at $h/p \sim 0.5$ nm. With a further increase of $h/p$, $\delta_{opt}$ varies periodically, which can be explained by the standing wave resonances in the finite-size parallel plate metallic waveguide formed by the Au-nanoridges.

Next, we optimized the thickness of an $Al_2O_3$-coating that entirely fills the gaps between the Au-nanoridges and serves as the antireflection coating. This coating ensures effective optical pump coupling into the photoconductor.[33] Figures 1 (e) and (f) show the results of this optimization and the EM field intensity distribution $I(x, y)$ for the optimal thickness of the $Al_2O_3$-antireflection coating of $d$= 180 nm, which reduces the Fresnel reflection down to ~ 5% thus allowing ~ 95% of the incident radiation to penetrate into the photoconductive substrate. With thus selected optimal parameters of the plasmonic grating ($h$= 100 nm, $w$= 100 nm, $p$= 200 nm, and $d$= 180 nm), we have confirmed numerically a significant field enhancement behind the plasmonic grating.

Next, we fabricated the optimized plasmonic and conventional THz PCAs. The conventional PCA utilized the same photoconductive substrate, log-spiral Au-electrodes with the gap of 10$\mu$m and the $Al_2O_3$-coating but did not feature the plasmonic gratings. The fabrication technique was similar to that reported in Ref. 34. First, we passivated the surface of a SI-GaAs photoconductor with a 230 nm $Si_3N_4$ dielectric layer, then we etched two windows near the photoconductive gap for the antenna/semiconductor contact, and then deposited 50/450-nm-thick Ti/Au PCA electrodes using electron-beam evaporation. The plasmonic gratings were formed by the electron-beam lithography with 18/82-nm-thick Ti/Au metallization followed by the lift-off process. Finally, the 10×10 $\mu m^2$ plasmonic grating was inscribed onto each of the two electrodes. Figure 2 shows the scanning electron microscopy (SEM) image illustrating the PCA structure, as well as the current-voltage characteristics demonstrating the reduction of the dark current $i_d$ in the passivated PCA. As shown in Figs. 3 (a) and (b), the two arrays of Au-nanoridges are attached to the corresponding antenna electrodes and are separated by the 10-$\mu$m-wide gap. Finally, the resultant photoconductive antenna was coated with a 180-nm-thick $Al_2O_3$-coating using the atomic-layer deposition. Figure 3 (c) shows the SEM image of the PCA cross-section illustrating that the $Al_2O_3$-coating penetrated the voids between the Au-nanoridges, thus helping to maintain the mechanical stability of the grating,[33] and enhancing the optical pump coupling into the PCA.[23,33] As seen from Fig. 3, the geometry of the fabricated plasmonic gratings corresponds to the one used in numerical modeling (see Fig. 1). It is also important to notice that the proposed passivation approach excludes mesa etching.[35] Therefore, it is suitable for any photoconductive material.

To experimentally characterize the fabricated PCAs, we used them as emitters in the THz-time-domain spectroscopy system (THz-TDS) measuring THz waveforms and THz power spectra $P_{THz}$. The THz-TDS is similar to the one used in our previous studies.[36,37] It uses the compact femtosecond fiber laser Toptica FemtoFErb780 featuring the central

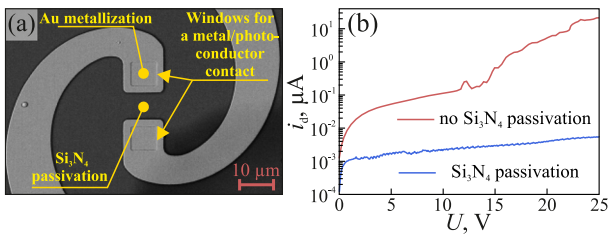


**FIG. 2**. Introduction of the passivation layer into PCA structure, and its impact on the dark current: (a) SEM image illustrating the photoconductive gap being passivated with a $Si_3N_4$-dielectric layer that features two windows to provide antenna/semiconductor contact; (b) dark current $i_d$ versus bias voltage $U$ for both passivated and non-passivated PCAs.

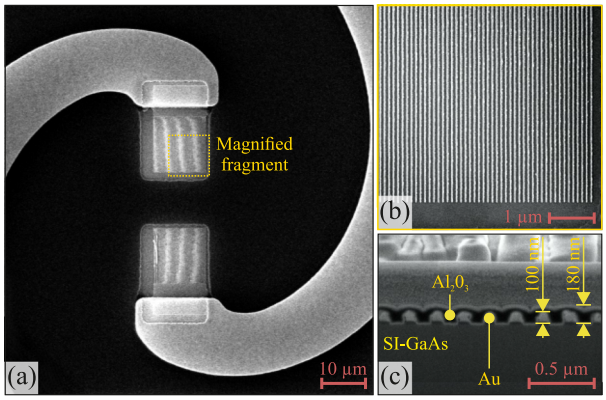


**FIG. 3**. Fabrication of the plasmon-assisted PCA: (a) SEM image of the passivated photoconductive gap, antenna metallization with the log-spiral Au-electrodes and two plasmonic gratings; (b) magnified image of the plasmonic grating; (c) SEM image of the plasmonic grating cross-section that shows the $Al_2O_3$ filling/coating, nanoridges, and their geometrical parameters.

wavelength of $\lambda$ = 0.78$\mu$m, the pulse repetition rate of $f$= 100 MHz, and the pulse duration of $\tau$= 95 fs. In our experiments, we biased the PCA emitters with U= 30 Volts and varied the optical pump power in the range of $P_{opt} \approx$ 0.1 to 10 mW using a set of attenuators. The emitted THz beam was collimated using a pair of the HRFZ-Si hemispheres and an off-axis gold parabolic mirror. The beam was then focused onto the PCA-detector (commercial THz receiver with a wrapped-dipole antenna topology, i.e. dipole with twisted bias lines) with the same optical components as used for the beam collimation. The PCA-emitter and the PCA-detector were placed in contact with the flat surfaces of the HRFZ-Si hemispheres. During comparative measurements, we only substituted and adjusted the PCA-emitters, while keeping the rest of the THz beam path unaltered. The time-independent THz photocurrent, i.e. the average photocurrent over THz pulse, was measured under fs laser illumination at bias voltage of 30 Volts for the plasmon-assisted ($i_{pl}$) and conventional PCAs ($i_c$), respectively.

Figure 4 (a) shows the normalized THz power spectra $P_{THz}/P_{opt}$ for both the plasmonic and conventional PCAs-emitters at high and low powers of the optical pump $P_{opt}$ = 10 mW and 1.0 mW, respectively. Figures 4 (c) and (d) show the THz photocurrent enhancement factor $\delta_i$ and the THz power enhancement factor $\delta_{THz}$ as a function of the optical pump power $P_{opt}$, where $\delta_i$ is defined as a ratio of the THz photocurrents of the plasmonic and conventional PCAs, while $\delta_{THz}$ is a ratio of integrals over the THz power spectrum for the two PCAs in the frequency domain calculated as follows:

$$\delta_i = \frac{i_{pl}}{i_c}, \qquad \delta_{THz} = \int P^{pl}_{THz}(\nu)d\nu \Big/ \int P^{c}_{THz}(\nu)d\nu. \tag{1}$$

where $P^{pl,c}_{THz}$ are the THz power spectra for the plasmon-assisted and conventional PCAs. We observe a strong

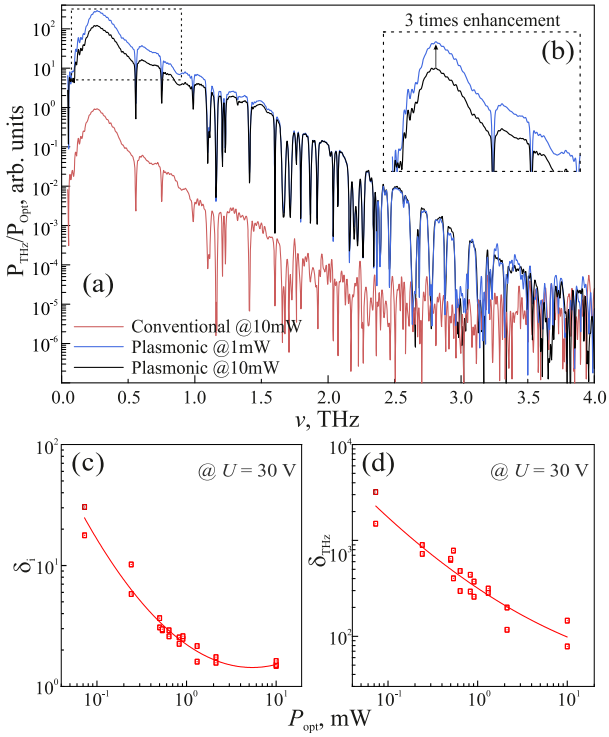


**FIG. 4**. Experimental comparison of the plasmon-assisted and conventional PCAs: (a) the normalized THz power spectra $P_{THz}/P_{opt}$ for various pump powers $P_{opt}$= 1 and 10 mW; (b) $P_{THz}/P_{opt}$ for the plasmonic PCA at various optical pump powers; (c), (d) the THz photocurrent enhancement factor $\delta_i$ and the THz power enhancement factor $\delta_{THz}$ as a function of the optical pump power $P_{opt}$.

enhancement in both the THz photocurrent and the THz power for the plasmon-assisted PCA compared to the conventional PCA. The highest THz power enhancement factor of $\delta_{THz}= 3 \times 10^3$ is observed at low powers of the optical pump $P_{opt} < 1.0$ mW. Figure 4 also shows the reduction in the THz generation enhancement when increasing the pump power $P_{opt}$. Namely, when increasing the optical pump power from 0.1 to 10 mW, the THz photocurrent enhancement decreases from $\delta_i$= 30 to 2 and the THz power enhancement decreases from $\delta_{THz}= 3 \times 10^3$ to $10^2$.

There could be a number of reasons for the observed reduction. First, with an increase in the pump power, we could expect broadening of the pump beam caustics formed behind the plasmonic nanoridges, thus, leading to an increase in the volume of the photoconductor occupied by the electron-hole plasma. Such an expansion of the electron-hole plasma volume could lead to a reduction in the efficiency of THz wave generation due to more pronounced charge screening effects.[38,39] Moreover, the enhancement of the electron-hole pairs generation deep in the semiconductor volume reduces the efficiency of the optical-to-THz-wave conversion, since only the photocarriers in a close proximity to the plasmonic grating contribute to the THz pulse generation.[11] A wide

bandgap semiconductor layer placed under the photo absorbing layer could reduce the electron-hole generation deeper into the semiconductor. The geometry and composition of such layer could be optimized by performing Monte Carlo simulations.[40] Additionally the increase of the PCA performance and its thermal stability can be reached by using short-carrier-lifetime semiconductors.[41]

In conclusion, we used the numerical simulations to optimize the plasmon-assisted PCA design, then fabricated and characterized the optimized plasmon-assisted PCA and confirmed a significant enhancement of the THz pulsed generation and its superior operation at low pump powers. The plasmon-assisted PCA uses the effect of the optical field confinement in the vicinity of the high-aspect-ratio dielectric-embedded Au-grating. Based on the achieved dynamic range of 70 dB, large spectral bandwidth of 4 THz, and low optical pump powers < 1 mW, we can claim that our plasmonic PCA competes well with the most advanced PCAs known to date based on optical nanoantennas, optical nanocavities, and other enhancement techniques.[14,42] It is also important to note that other known plasmonic PCAs utilizing the same photoconductive substrate SI-GaAs with different metal adhesion layers[43] or polarization insensitive designs[17] do not reach as high dynamic range or bandwidth as our antenna. A large $3 \times 10^3$-times enhancement of the THz beam power generation at low optical pump powers reveals strong potential of the plasmonic PCA for operation with low-power lasers. The developed numerical simulation approach and plasmonic fabrication technology could be also applied for the development of the electrically driven THz plasmonic detectors and sources.[44]

The work was supported by the Russian Scientific Foundation, Project # 18-79-10195. Prof. Skorobogatiy would like to acknowledge financial support from the Canada Research Chair I program in "Ubiquitous THz photonics." The work at RPI was supported by the Office of Naval Research, USA (Project Monitor Dr Paul Maki) and by the US Army Research Laboratory (Project Monitor Dr Meredith Reed).

## REFERENCES

[1] Y.-S. Lee, *Principles of Terahertz Science and Technology* (Springer, New York, NY, USA, 2009).
[2] P. Uhd Jepsen, R. Jacobsen, and S. Keiding, Journal of the Optical Society of America B **13**, 2424 (1996).
[3] C. Berry and M. Jarrahi, Journal of Infrared, Millimeter, and Terahertz Waves **33**, 1182 (2012).
[4] S.-H. Yang and M. Jarrahi, Applied Physics Letters **107**, 131111 (2015).
[5] S. Preu, G. H. Dohler, S. Malzer, L. J. Wang, and A. C. Gossard, J. Appl. Phys. **109**, 061301 (2011).
[6] D. Auston, Applied Physics Letters **26**, 101 (1975).
[7] E. Castro-Camus and M. Alfaro, Photonics Research **4**, A36 (2016).
[8] R. Leyman, A. Gorodetsky, N. Bazieva, G. Molis, A. Krotkus, E. Clarke, and E. Rafailov, Laser and Photonics Reviews **10**, 772 (2016).
[9] N. M. Burford and M. O. El-Shenawee, Optical Engineering **56**, 010901 (2017).
[10] C. Berry and M. Jarrahi, New Journal of Physics **14**, 105029 (2012).
[11] C. Berry, N. Wang, M. Hashemi, M. Unlu, and M. Jarrahi, Nature Communications **4**, 1622 (2013).
[12] B.-Y. Hsieh and M. Jarrahi, Journal of Applied Physics **109**, 084326 (2011).
[13] S.-H. Yang and M. Jarrahi, Optics Letters **38**, 3677 (2013).
[14] S. Lepeshov, A. Gorodetsky, A. Krasnok, E. Rafailov, and P. Belov, Laser and Photonics Reviews **11**, 1600199 (2016).
[15] S.-G. Park, Y. Choi, Y.-J. Oh, and K.-H. Jeong, Optics Express **20**, 25530 (2012).
[16] Y.-J. Oh and K.-H. Jeong, Advanced Materials **24**, 2234 (2012).
[17] X. Li, N. T. Yardimci, and M. Jarrahi, AIP Advances **7**, 115113 (2017).
[18] F. Miyamaru, Y. Saito, M. W. Takeda, L. Liu, B. Hou, W. Wen, and P. Sheng, Appl.Phys.Lett. **95**, 221111 (2009).
[19] C. Berry, M. Hashemi, and M. Jarrahi, Applied Physics Letters **104**, 081122 (2014).
[20] C. Berry, M. Hashemi, S. Preu, H. Lu, A. Gossard, and M. Jarrahi, Applied Physics Letters **105**, 011121 (2014).
[21] C. Berry, M. Hashemi, S. Preu, H. Lu, A. Gossard, and M. Jarrahi, Optics Letters **39**, 4522 (2014).
[22] O. Mitrofanov, Z. Han, F. Ding, S. Bozhevolnyi, I. Brener, and J. Reno, Applied Physics Letters **110**, 061109 (2017).
[23] T. Yardimci, S. Cakmakyapan, S. Hemmati, and M. Jarrahi, Scientific Reports **7**, 4166 (2017).
[24] N. Yardimci and M. Jarrahi, Scientific Reports **7**, 42667 (2017).
[25] O. Mitrofanov, I. Brener, T. S. Luk, and J. L. Reno, ACS Photonics **2**, 1763 (2015).
[26] S. Lepeshov, A. Gorodetsky, A. Krasnok, N. Toropov, T. A. Vartanyan, P. Belov, A. Alu, and E. Rafailov, Scientific Reports **8**, 6624 (2018).
[27] O. Mitrofanov, T. Siday, R. Thompson, T. Luk, I. Brener, and J. Reno, APL Photonics **3**, 051703 (2018).
[28] L. Edsberg, *Introduction to Computation and Modeling for Differential Equations* (Wiley, Hoboken, New Jersey, 2008).
[29] I. A. Glinskiy, N. V. Zenchenko, and P. P. Maltsev, Russian Technological Journal **4**, 27 (2016).
[30] D. Rakic and M. L. Majewski, J. Appl. Phys. **80**, 5909 (1996).
[31] M. A. Ordal, L. L. Long, R. J. Bell, S. E. Bell, R. R. Bell, R. W. Alexander, Jr., and C. A. Ward, Applied Optics **22**, 1099 (1983).
[32] M. R. Querry, Contractor Report CRDC-CR-85034 (1985).
[33] A. Gupta, G. Rana, A. Bhattacharya, A. Singh, R. Jain, R. Bapat, S. Duttagupta, and S. Prabhu, APL Photonics **3**, 051706 (2018).
[34] D. Ponomarev, R. Khabibullin, A. Yachmenev, A. Pavlov, D. Slapovskiy, I. Glinskiy, D. Lavrukhin, O. Ruban, and P. Maltsev, Semiconductors **51**, 1218 (2017).
[35] H. Roehle, R. Dietz, H. Hensel, J. Bottcher, H. Kunzel, D. Stanze, M. Schell, and B. Sartorius, Optics Express **18**, 2296 (2010).
[36] D. Lavrukhin, R. Khabibullin, A. Yachmenev, A. Pavlov, Y. Goncharov, I. Spektor, G. Komandin, S. Yurchenko, N. Chernomyrdin, K. Zaytsev, and D. Ponomarev, Semiconductor Science and Technology (2018, Under Review).
[37] G. M. Katyba, K. I. Zaytsev, N. V. Chernomyrdin, I. A. Shikunova, G. A. Komandin, V. B. Anzin, S. P. Lebedev, I. E. Spektor, V. E. Karasik, S. O. Yurchenko, I. V. Reshetov, V. N. Kurlov, and M. Skorobogatiy, Advanced Optical Materials **0**, 1800573.
[38] G. C. Loata, M. D. Thomson, T. Löffler, and H. G. Roskos, Applied Physics Letters **91**, 232506 (2007).
[39] Z. Piao, M. Tani, and K. Sakai, Japanese Journal of Applied Physics **39**, 96 (2000).
[40] M. Ryzhii, M. Willander, I. Khmyrova, and V. Ryzhii, J. Appl. Phys. **84**, 6419 (1998).
[41] M. R. Stone, M. Naftaly, R. E. Miles, J. R. Fletcher, and D. P. Steenson, IEEE Transactions on Microwave Theory and Techniques **52**, 2420 (2004).
[42] N. T. Yardimci and M. Jarrahi, Small, 1802437.
[43] D. Turan, S. C. Corzo-Garcia, N. T. Yardimci, E. Castro-Camus, and M. Jarrahi, Journal of Infrared, Millimeter, and Terahertz Waves **38**, 1448 (2017).
[44] M. Shur, Proc. SPIE **10639**, 1063907 (2018).